

de Sitter extremal surfaces

K. Narayan

*Chennai Mathematical Institute,
SIPCOT IT Park, Siruseri 603103, India.*

Abstract

We study extremal surfaces in de Sitter space in the Poincare slicing in the upper patch, anchored on spatial subregions at the future boundary \mathcal{I}^+ , restricted to constant boundary Euclidean time slices (focussing on strip subregions). We find real extremal surfaces of minimal area as the boundaries of past lightcone wedges of the subregions in question: these are null surfaces with vanishing area. We also find complex extremal surfaces as complex extrema of the area functional, and the area is not always real-valued. In dS_4 the area is real. The area has structural resemblance with entanglement entropy in a dual *CFT*. There are parallels with analytic continuation from the Ryu-Takayanagi expressions for holographic entanglement entropy in *AdS*. We also discuss extremal surfaces in the *dS* black brane and the de Sitter “bluewall” studied previously. The dS_4 black brane complex surfaces exhibit a real finite cutoff-independent extensive piece. In the bluewall geometry, there are real surfaces that go from one asymptotic universe to the other through the Cauchy horizons.

Contents

1	Introduction	1
2	Extremal surfaces in de Sitter space	3
2.1	Real extremal surfaces	3
2.2	Complex extremal surfaces	6
3	Extremal surfaces in the dS black brane	12
3.1	The de Sitter bluewall	14
4	Discussion	16

1 Introduction

de Sitter space is fascinating for many reasons, in particular for holographic explorations towards addressing questions of cosmology and time. In this regard, some versions of dS/CFT duality [1, 2, 3] associate to de Sitter space a dual Euclidean CFT on the future timelike infinity \mathcal{I}^+ boundary (in the Poincare slicing). A concrete realization in the context of higher spin theories appears in [4]. Further work on dS/CFT appears in *e.g.* [5, 6, 7, 8, 9, 10, 11, 12, 13].

In AdS/CFT , there has been considerable interest in understanding information theoretic notions in terms of geometric quantities via holography, in particular stemming from the Ryu-Takayanagi prescription [14, 15] (see [16, 17] for reviews) for calculating holographic entanglement entropy of a subsystem in the strongly coupled boundary field theory. This is the area of a bulk minimal surface (in Planck units) anchored at the subsystem interface and dipping inwards upto a certain maximal depth typically called the turning point. A different way to think about this appears in [18]. More generally, these are extremal surfaces [19]. In this light, one might speculate that the bulk subregion enclosed by the entangling surface and the boundary subsystem in some sense encodes bulk physics corresponding to that part of the boundary theory contained in the subsystem, although a detailed understanding of the hologram (and bulk locality) would seem more intricate.

It is interesting to consider these questions in the context of de Sitter space and dS/CFT . Assuming there is translation invariance with respect to a boundary Euclidean time direction, imagine constructing a subregion on a Euclidean time slice of the future boundary \mathcal{I}^+ . Tracing out the complement of this subregion would lead to some loss of information and thereby give some associated entropy, which one might attribute to the subregion being entangled with the complement. In the bulk, intuition from the Ryu-Takayanagi prescription in AdS/CFT suggests that we study extremal surfaces in de Sitter space (in the Poincare slicing) on a constant boundary Euclidean time slice, defined as anchored on the subregion on the future (spacelike) boundary and dipping inwards (*i.e.* in the bulk time direction, towards the past). We find (sec. 2) that the bulk extremization problem exhibits some crucial sign differences from the AdS case. Focussing first on real surfaces, there are correspondingly some technical differences

such as the absence of a natural turning point (where the surface stops dipping inward). For sufficiently symmetric subregions such as strips (with an axis of symmetry), extremal surfaces can be defined as the union of two half-extremal-surfaces joined continuously but with a sharp cusp. Upon requiring that we choose minimal area, the extremal surfaces become null surfaces with zero area. In fact these are simply the boundaries of the past lightcone wedges of the subregion in question (restricted to the boundary Euclidean time slice), and are thus analogous to the causal wedges associated with causal holographic information [20] (note that these bulk causal wedges and the corresponding causal holographic information in general do not coincide with the bulk entangling subregion, and entanglement entropy). This answer – restrictions of past lightcone wedges – is well-defined for arbitrary boundary subregions, even without sufficiently high symmetry, and gives vanishing area. These surfaces with vanishing area do not appear to have any connection to entanglement in dS/CFT .

It is therefore interesting to look for other extrema, in particular complex saddle points of the extremization problem, motivated by considerations in dS/CFT . For instance, in the formulation of [3] of the dS/CFT dictionary, the CFT partition function is $Z_{CFT} = \Psi$ where Ψ is the bulk late time Hartle-Hawking wavefunction of the universe subject to appropriate (Bunch-Davies) boundary conditions at early times. In a semiclassical approximation $\Psi \sim e^{iS_{cl}}$, the dual CFT energy-momentum tensor $\langle TT \rangle$ correlators exhibit central charge coefficients of the form $\mathcal{C}_d \sim i^{1-d} \frac{R_{dS}^{d-1}}{G_{d+1}}$ (which is essentially an analytic continuation from Euclidean AdS_{d+1}). With this in mind, focussing again on strip subregions in the present context, we indeed find these complex extremal surfaces: they exhibit “turning points” in the interior. They should be thought of as living in some auxiliary space, and are distinct from the bulk past lightcone wedges (which define real subregions in bulk dS_4). The area of these surfaces is in general not real-valued. In dS_4 , we find that $x(\tau)$ parametrizing the strip width being real-valued suggests that the bulk time τ parametrizes a complex path $\tau = iT$. The area (in Planck units) of these complex surfaces in dS_4 is real-valued and negative, while in dS_{d+1} with d even, the nature of these surfaces is different and the area is pure imaginary. The area has structural resemblance with entanglement entropy in a dual (non-unitary) CFT_d , with central charge $\mathcal{C}_d \sim i^{1-d} \frac{R_{dS}^{d-1}}{G_{d+1}}$, with a leading area law divergence, and subleading terms. There are parallels with analytic continuation from the Ryu-Takayanagi holographic entanglement expressions from AdS . It is a useful consistency check that these central charges $\mathcal{C}_d \sim i^{1-d} \frac{R_{dS}^{d-1}}{G_{d+1}}$ here resemble those in the $\langle TT \rangle$ correlators in [3], mentioned above. From the point of view of the dual Euclidean CFT living on the future boundary \mathcal{I}^+ , one might formally associate a density matrix w.r.t. boundary Euclidean time evolution and a reduced density matrix to the subregion obtained by tracing out the complement. It would be interesting to explore this further, perhaps in dS/CFT as entanglement entropy in the dual Euclidean CFT.

We then discuss (sec. 3) an asymptotically de Sitter space [13] – the dS black brane –

where subleading normalizable metric components are turned on: in dS_4/CFT_3 , they have the interpretation of saddle points representing the Euclidean CFT with uniform energy-momentum density expectation value. The corresponding extremal surfaces in the dS_4 black brane exhibit a finite cutoff-independent real-valued extensive piece (again negative) with some resemblance to a thermal entropy. Finally we discuss (real) extremal surfaces in the closely related dS “bluewall” geometry, which are not obtained by analytic continuation: there are real extremal surfaces which cross from one asymptotic universe to the other through the Cauchy horizons.

2 Extremal surfaces in de Sitter space

de Sitter space dS_{d+1} in the Poincare slicing or planar coordinate foliation is given by the metric

$$ds^2 = \frac{R_{dS}^2}{\tau^2}(-d\tau^2 + dw^2 + dx_i^2), \quad (1)$$

where half of the spacetime, *e.g.* the upper patch, has \mathcal{I}^+ at $\tau = 0$ and a coordinate horizon at $\tau = -\infty$. This may be obtained by analytic continuation of a Poincare slicing of AdS ,

$$r \rightarrow -i\tau, \quad R_{AdS} \rightarrow -iR_{dS}, \quad t \rightarrow -iw, \quad (2)$$

where w is akin to boundary Euclidean time, continued from time in AdS .

The dual Euclidean CFT is taken as living on the future $\tau = 0$ boundary \mathcal{I}^+ . We assume translation invariance with respect to a boundary Euclidean time direction, say w , and consider a subregion on a $w = \text{const}$ slice of \mathcal{I}^+ . One might imagine that tracing out the complement of this subregion then gives entropy in some sense stemming from the information lost. In the bulk, we study de Sitter extremal surfaces on the $w = \text{const}$ slice, analogous to the Ryu-Takayanagi prescription in AdS/CFT . Operationally these extremal surfaces begin at the interface of the subsystem (or subregion) and dip inwards (towards the past, in the bulk time direction). For simplicity, consider a strip on the $w = \text{const}$ surface (*i.e.* a constant boundary Euclidean time surface): this bulk d -dim subspace has metric

$$ds^2 = \frac{R_{dS}^2}{\tau^2} \left(-d\tau^2 + \sum_{x_i \neq w} dx_i^2 \right). \quad (3)$$

This is not a spacelike subspace in the bulk and it might seem that the extremal surfaces are timelike in general: however we will find that this is not the case.

2.1 Real extremal surfaces

Let us consider a strip subregion with width direction say x , the remaining x_i being labelled y_i . A bulk surface on the $w = \text{const}$ slice bounding this subregion and dipping inward (towards

the past) is bulk codim-2: its area functional in Planck units is

$$S_{dS} = \frac{1}{4G_{d+1}} \int \prod_{i=1}^{d-2} \frac{R_{dS} dy_i}{\tau} \frac{R_{dS}}{\tau} \sqrt{d\tau^2 - dx^2} = \frac{R_{dS}^{d-1} V_{d-2}}{4G_{d+1}} \int \frac{d\tau}{\tau^{d-1}} \sqrt{1 - \left(\frac{dx}{d\tau}\right)^2}. \quad (4)$$

We consider extremizing the action to find extremal surfaces with minimal area, along the lines of the Ryu-Takayanagi prescription for entanglement entropy in AdS . The S_{dS} extremization gives a conserved quantity ($\dot{x} \equiv \frac{dx}{d\tau}$)

$$-\frac{\dot{x}}{\sqrt{1-\dot{x}^2}} = B\tau^{d-1} \quad \Rightarrow \quad 1 - \dot{x}^2 = \frac{1}{1 + B^2\tau^{2d-2}} \quad i.e. \quad \dot{x}^2 = \frac{B^2\tau^{2d-2}}{1 + B^2\tau^{2d-2}}. \quad (5)$$

We see that $\dot{x}^2 \rightarrow 0$ near the boundary $\tau \rightarrow 0$. Assuming the conserved constant satisfies $B^2 > 0$ makes all the expressions real-valued and means $\dot{x}^2 > 0$, with $\dot{x}^2 \rightarrow 1$ in the deep interior for large $|\tau|$. For $B^2 > 0$, these are timelike surfaces¹. This gives the solution (upto boundary conditions) and corresponding area integral

$$x(\tau) = \pm \int \frac{B\tau^{d-1} d\tau}{\sqrt{1 + B^2\tau^{2d-2}}} \equiv \pm X(\tau), \quad S_{dS} = \frac{R_{dS}^{d-1}}{4G_{d+1}} V_{d-2} \int_{\epsilon}^{\tau_0} \frac{d\tau}{\tau^{d-1}} \frac{1}{\sqrt{1 + B^2\tau^{2d-2}}}. \quad (6)$$

The main difference between this case and the minimal surface in AdS stems from $B^2 > 0$ implying that there is no smooth ‘‘turning point’’ where $\dot{x}^2 = \frac{B^2\tau^{2d-2}}{1+B^2\tau^{2d-2}} \rightarrow \infty$. In fact $B^2 > 0$ means \dot{x}^2 is bounded, with $0 \leq \dot{x}^2 \leq 1$. For any finite $B^2 > 0$, the extremal surface in this case begins to dip inwards from one boundary of the strip subregion and (rather than turning around as in AdS) continues indefinitely, eventually approaching $\dot{x} \rightarrow \pm 1$. With a view to associating a bulk subregion with the boundary subregion in question, let us artificially cut off the inward dipping surface at some interior location $\tau = \tau_0$, the bulk subregion then defined by the interior of the boundary strip subregion and the joined surface. So consider the half-extremal-surfaces,

$$\begin{aligned} x_L(\tau) &= X(\tau) - X(\tau_0) = -x_R(\tau), \\ x_L(\tau_0) &= 0 = x_R(\tau_0), \quad x_L(0) = -\frac{l}{2} = -x_R(0) \quad \Rightarrow \quad \frac{l}{2} = X(\tau_0). \end{aligned} \quad (7)$$

This gives an extremal surface made of two half-extremal-surfaces joined continuously but with a sharp cusp at τ_0 (see Figure 1). This defines the corresponding wedge-like bulk subregion, enclosed by this extremal surface and the boundary subregion. These conditions do not determine the parameters B, τ_0 uniquely, given the subregion width l . Varying B gives different extremal surfaces. By comparison, in the AdS case, the turning point $\tau_* = \frac{1}{B}$ is fixed by the global nature of the entangling surface as the location where $\dot{x}^2 \rightarrow \infty$, the surface turning around.

¹One might instead want to consider spacelike surfaces with $\dot{x}^2 > 1$ and therefore take, instead of (4), the area functional as $S_{dS} = \frac{R_{dS}^{d-1} V_{d-2}}{4G_{d+1}} \int \frac{d\tau}{\tau^{d-1}} \sqrt{\left(\frac{dx}{d\tau}\right)^2 - 1}$. We will discuss this in the next subsection.

To follow the Ryu-Takayanagi prescription, we would want to identify those extremal surfaces that have minimal area². From (6), we see that as B increases, the area S_{dS} decreases. Furthermore, (5) shows that as B increases, \dot{x}^2 increases and eventually approaches $\dot{x}^2 \rightarrow 1$ as $B \rightarrow \infty$. In this limit, $x(\tau) \rightarrow \pm\tau$ and S_{dS} appears to vanish. In fact this is a sensible result: in hindsight, it should have been obvious from (4) that minimal area arises when the extremal surface becomes null. This null extremal surface is in fact simply the boundary of the past bulk lightcone of the subregion, restricted to the boundary Euclidean time slice.

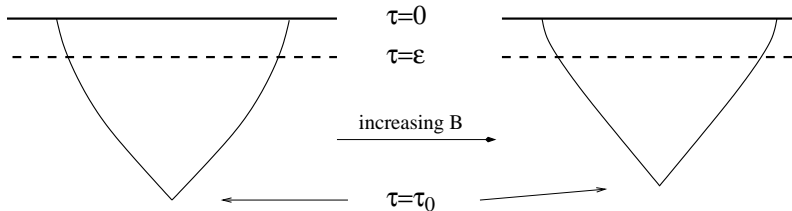


Figure 1: Extremal surfaces in de Sitter made of two half-extremal surfaces joined continuously but with a sharp cusp at τ_0 . As B increases (till eventually $B \gg \frac{1}{\epsilon^{d-1}}$), the surface approaches $\dot{x}^2 \rightarrow 1$ (figure on the right).

An alternative argument corroborating the above conclusion is the following. Physically, the shortest length (or time) scale here is $\tau_{UV} = \epsilon$ so that in (5) when $B\epsilon^{d-1} \gg 1$ we can approximate $\dot{x}^2 \sim 1$ and so $x(\tau) \sim \pm\tau$ giving $\frac{l}{2} \sim \tau_0$. Thus one might estimate (6) as

$$S_{dS} \sim \frac{R_{dS}^{d-1}}{4G_{d+1}} V_{d-2} \int_{\epsilon}^{\tau_0} \frac{d\tau}{\tau^{d-1}} + \frac{R_{dS}^{d-1}}{4G_{d+1}} V_{d-2} \int_0^{\tau_0} \frac{d\tau}{\tau^{d-1}} \left(\frac{1}{\sqrt{1+B^2\tau^{2d-2}}} - 1 \right), \quad (8)$$

where the second integral can be seen to vanish as $\tau \rightarrow 0$. Now the first integral scales as $\frac{V_{d-2}}{\epsilon^{d-2}}$ while the second integral can be expressed in terms of the hypergeometric function ${}_2F_1$ as $\frac{R_{dS}^{d-1}}{G_{d+1}} \frac{V_{d-2}}{(d-2)\tau_0^{d-2}} [1 - {}_2F_1(\frac{1}{2}, -\frac{d-2}{2(d-1)}, \frac{d}{2(d-1)}, -B^2\tau_0^{2d-2})]$ (the extremal surface in (6) is itself expressed as $x(\tau) = \pm\tau {}_2F_1(\frac{1}{2}, \frac{1}{2-2d}, \frac{3-2d}{2-2d}, -\frac{1}{B^2\tau^{2d-2}})$ or $\pm B\tau^d {}_2F_1(\frac{1}{2}, \frac{d}{2d-2}, \frac{3d-2}{2d-2}, -B^2\tau^{2d-2})$, using the integral representations of ${}_2F_1$). As B^2 increases, this second integral is seen to scale as $-\frac{R_{dS}^{d-1}}{G_{d+1}} V_{d-2} B^{(d-2)/(d-1)}$. Thus when $B \sim \frac{1}{\epsilon^{d-1}}$ this cancels the earlier contribution and we again see the leading S_{dS} scaling to be vanishing.

In dS_3 (*i.e.* $d = 2$), we obtain $x(\tau) = \pm \int \frac{B\tau d\tau}{\sqrt{1+B^2\tau^2}} = \pm \frac{1}{B} \sqrt{1+B^2\tau^2}$ and the boundary conditions give $\frac{1}{B}(\sqrt{1+B^2\tau_0^2} - 1) = \frac{l}{2}$, the area integral becoming $S_{dS} = \frac{R_{dS}}{4G_3} \int_{\epsilon}^{\tau_0} \frac{d\tau}{\tau \sqrt{1+B^2\tau^2}}$. Analysing these vindicates the conclusions above.

It is worth noting that our construction of joining two half-extremal-surfaces appears invalid unless the subsystem has sufficiently high symmetry (in particular an axis of symmetry). Relatedly, one might look askance at the entire extremization procedure here, in particular whether

²Note that surfaces with maximum area correspond to minimizing B : this gives $B = 0$, which are disconnected surfaces $x(\tau) = const$, with area $S_{dS} \sim \frac{R_{dS}^{d-1}}{4G_{d+1}} V_{d-2} \int_{\epsilon}^{\tau_0} \frac{d\tau}{\tau^{d-1}}$ with a leading divergent piece.

one allows non-smooth surfaces (with cusps) in the extremization: one might then wonder if more general surfaces need to be considered, *e.g.* a zigzag null surface formed by joining multiple partial surfaces with multiple cusps. This would be useful to systematise more rigorously. However the final answer, the past lightcone wedge, is well-defined for an arbitrary subregion, comprising two piecewise smooth extremal surfaces joined with just a single cusp (rather than multiple cusps). The past lightcone wedge boundary (restricted to the boundary Euclidean time slice) is however a complicated surface: it would be interesting to understand the shape dependence here. The resulting area is of course always zero for all these null surfaces, and does not reflect entanglement structure.

From the point of view of bulk de Sitter alone, one could consider volume subregions in the full d -dim boundary \mathcal{I}^+ (at $\tau = 0$), *i.e.* not on the constant boundary Euclidean time slice. These would give codim-1 surfaces. For a strip subregion with width direction say x , the remaining x_i being labelled y_i , analysing the area integral of the bulk surface for extremization gives

$$\begin{aligned}
S_{dS} &\sim R_{dS}^d V_{d-1} \int \frac{d\tau}{\tau^d} \sqrt{1 - \left(\frac{dx}{d\tau}\right)^2}, & -\frac{\dot{x}}{\sqrt{1-x^2}} &= B\tau^d, \\
\Rightarrow \dot{x}^2 &= \frac{B^2\tau^{2d}}{1+B^2\tau^{2d}}, & S_{dS} &= R_{dS}^d V_{d-1} \int_{\epsilon}^{\tau_0} \frac{d\tau}{\tau^d} \frac{1}{\sqrt{1+B^2\tau^{2d}}}.
\end{aligned} \tag{9}$$

This has volume scaling. Again S_{dS} decreases with increasing B , with $\dot{x}^2 \rightarrow 1$: the resulting extremal surfaces are null surfaces defining the past lightcone wedges of the volume subregion, with vanishing area.

These real null surfaces with vanishing area do not appear to have any bearing on entanglement in dS/CFT . In what follows, we will explore other complex saddle points.

2.2 Complex extremal surfaces

For what follows, it is useful to recall the dS/CFT correspondence, for de Sitter space in the Poincare slicing (1), obtained by analytic continuation (2) of Poincare AdS . A version of dS/CFT [1, 2, 3] states that quantum gravity in de Sitter space is dual to a Euclidean CFT living on the future boundary \mathcal{I}^+ . More specifically, the CFT partition function with specified sources $\phi_{i0}(\vec{x})$ coupled to operators \mathcal{O}_i is identified [3] with the bulk Hartle-Hawking “wave-function of the universe” as a functional of the boundary values of the fields dual to \mathcal{O}_i given by $\phi_{i0}(\vec{x})$. In a semiclassical approximation, this becomes $Z_{CFT} = \Psi[\phi_{i0}(\vec{x})] \sim e^{iS_{cl}[\phi_{i0}]}$ where we need to impose regularity conditions on the past cosmological horizon $\tau \rightarrow -\infty$: *e.g.* scalar modes satisfy $\phi_k(\tau) \sim e^{ik\tau}$, which are Hartle-Hawking (or Bunch-Davies) initial conditions. Operationally, certain dS/CFT observables can be obtained by analytic continuation (2) from AdS (see *e.g.* [3], as well as [5]). The Bunch-Davies initial condition itself can be thought

of as analytic continuation of regularity in the AdS interior. Dual CFT correlation functions can be obtained from the dictionary $Z_{CFT} = \Psi$. For instance (from [3]) in a semiclassical approximation $\Psi \sim e^{iS_{cl}}$, a massless scalar in dS_4 has a mode solution $\phi = \phi_{\vec{k}}^0 \frac{(1-ik\tau)e^{ik\tau}}{(1-ik\tau_c)e^{ik\tau_c}}$ with Bunch-Davies initial conditions $\phi \sim e^{ik\tau}$ at early times ($|\tau| \rightarrow \infty$) and τ_c a late-time cutoff. The classical action evaluated on this solution is $iS_{dS_4} \sim \frac{R_{dS}^2}{G_4} \int d^3k (i\frac{k^3}{\tau_c} - k^3 + \dots) \phi_{-\vec{k}}^0 \phi_{\vec{k}}^0$, the divergent terms being oscillatory (pure imaginary). Appropriate graviton modes can be approximated as massless scalars so that dual CFT energy-momentum tensor $\langle TT \rangle$ correlators can be read off as $\langle T(\vec{k})T(\vec{k}') \rangle_{dS_4} = \frac{\delta^2 Z_{CFT}}{\delta\phi_{\vec{k}}^0 \delta\phi_{\vec{k}'}^0} |_{\phi^0=0} \sim (-\frac{R_{dS}^2}{G_4}) k^3 \delta(\vec{k} + \vec{k}')$. The central charge coefficient here is $\mathcal{C}_4 \sim -\frac{R_{dS}^2}{G_4}$ essentially an analytic continuation from Euclidean AdS_4 . In dS_5 [3], we have $iS_{dS_5} \sim i\frac{R_{dS}^3}{G_5} \int d^4k \phi_{-\vec{k}}^0 \phi_{\vec{k}}^0 (\dots + k^4 \log(-\tau_c k) + \dots)$ where we have only exhibited the nonlocal term which contributes to the 2-point function: this gives $\langle T(\vec{k})T(\vec{k}') \rangle_{dS_5} \sim (i\frac{R_{dS}^3}{G_5}) k^4 \log k \delta(\vec{k} + \vec{k}')$, with central charge coefficient $\mathcal{C}_5 \sim i\frac{R_{dS}^3}{G_5}$. More generally we have $\mathcal{C}_d \sim i^{1-d} \frac{R_{dS}^{d-1}}{G_{d+1}}$ (which is essentially an analytic continuation from $EAdS_{d+1}$).

From this dS/CFT point of view, one might expect any leading divergence in the CFT entanglement entropy (assuming it exists) to be of the form $\mathcal{C}_d \frac{V_{d-2}}{\epsilon^{d-2}}$ which is in general complex-valued: thus it is natural to ask if there are additional (perhaps complex³) extrema of the area functional that should be considered in de Sitter space, with possible dS/CFT interpretations. With a view to considering spacelike surfaces with $\dot{x}^2 > 1$, let us take, instead of (4), the dS_{d+1} area functional on a $w = const$ slice as

$$S_{dS} = \frac{R_{dS}^{d-1} V_{d-2}}{4G_{d+1}} \int \frac{d\tau}{\tau^{d-1}} \sqrt{\left(\frac{dx}{d\tau}\right)^2 - 1}, \quad \frac{\dot{x}}{\sqrt{\dot{x}^2 - 1}} = A\tau^{d-1}, \quad (10)$$

where we are considering strip subsystems with width along x . The second expression above is the conserved quantity obtained in the extremization. This is essentially the same as (5), but with $B^2 = -A^2 < 0$, and A being real. One might ask if this can be interpreted as a real surface $\dot{x}^2 = \frac{A^2 \tau^{2d-2}}{A^2 \tau^{2d-2} - 1}$. However we need to require that the surface reaches the boundary $\tau \rightarrow 0$ from where it drops down (inward): near $\tau \rightarrow 0$, we find $\dot{x}^2 \sim -A^2 \tau^{2d-2}$, so that

$$\dot{x}^2 = \frac{-A^2 \tau^{2d-2}}{1 - A^2 \tau^{2d-2}}, \quad (11)$$

this being a complex surface in some sense.

Let us focus now on dS_4/CFT_3 for concreteness, to understand this better. The extremal surface near $\tau \rightarrow 0$ in this case is $x(\tau) \sim \pm iA\tau^3 + x(0)$. We want $x(\tau)$ to be real-valued since it parametrizes a space direction in the dual CFT_3 : this requires that τ takes imaginary values. In more detail, near $\tau \rightarrow 0$, we have $x \rightarrow \pm \frac{l}{2}$ and the two ends of the surface are parametrized

³Recall that complex geodesics appeared in [21] in the context of the black hole interior. Complex extremal surfaces have recently appeared in a different context [22], as well as [23].

as $x_L(\tau) \sim -\frac{l}{2} + iA\tau^3$ and $x_R(\tau) \sim \frac{l}{2} - iA\tau^3$. For $x_{L,R}$ to be real-valued with A real, we must have pure imaginary $\tau = iT$ with T real, giving $x_L \sim -\frac{l}{2} + AT^3 \sim -x_R$: as T increases, x_L increases from $-\frac{l}{2}$ and x_R decreases from $\frac{l}{2}$. The global structure of the surface shows a “turning point” at $\tau_*^4 A^2 = 1$, where $\dot{x}^2 \rightarrow \infty$, very similar to the situation in AdS . From the point of view of the discussion in the previous subsection, the two half-extremal-surfaces x_L, x_R in this case join smoothly at the turning point τ_* as in AdS , with $x_L(\tau_*) = 0 = x_R(\tau_*)$ and \dot{x}_L, \dot{x}_R matching. This gives the width

$$\frac{\Delta x}{2} = \frac{l}{2} = i \int_0^{\tau_*} \frac{A\tau^2 d\tau}{\sqrt{1-A^2\tau^4}} \xrightarrow{\tau=iT} \int_0^{T_*} \frac{i \cdot i^3 \cdot AT^2 dT}{\sqrt{1-A^2T^4}} = \#T_* \Rightarrow \tau_* \sim il. \quad (12)$$

The reality of $\Delta x = l$ with A real again suggests that we parametrize the τ -integral over the path $\tau = iT$ in a complex τ -plane⁴: we have then rescaled T using A to make the integration variable dimensionless (and $\# = \int_0^1 \frac{y^2 dy}{\sqrt{1-y^4}} = \sqrt{\pi} \frac{\Gamma(\frac{3}{4})}{\Gamma(\frac{1}{4})}$). The turning point here is $\tau_* = \frac{i}{\sqrt{A}}$. The integral can be parametrized in terms of hypergeometric functions ${}_2F_1$. The extremal surface $x(\tau)$ with τ imaginary does not correspond to any real bulk subregion in dS_4 enclosed by the surface, but really lives in some auxiliary space. In a sense, the structure here is very much like analytic continuation of the AdS_4 expressions a la Ryu-Takayanagi: we will discuss this more below. From that point of view, since the analytic continuation (2) faithfully maps $AdS_4 \leftrightarrow dS_4$, this is a faithful map from the subsystem to the auxiliary bulk subregion. The area now becomes

$$S_{dS} = 2 \frac{R_{dS}^2}{4G_4} V_1 \int_{\tau_{UV}}^{\tau_*} \frac{d\tau}{\tau^2} \frac{1}{\sqrt{A^2\tau^4 - 1}} = -i \frac{R_{dS}^2}{4G_4} V_1 \int_{\tau_{UV}}^{\tau_*} \frac{d\tau}{\tau^2} \frac{2}{\sqrt{1 - A^2\tau^4}}. \quad (13)$$

In principle, we could assign $\pm i$ in the second expression, as a choice of the branch of the square root: the choice of the minus sign leads to an appropriate coefficient as we see below. The integral itself is just as in AdS_4 , giving

$$S_{dS} = -i \frac{R_{dS}^2}{2G_4} V_1 \left(\frac{1}{\tau_{UV}} - c_3 \frac{1}{\tau_*} \right) = -\frac{R_{dS}^2}{2G_4} V_1 \left(\frac{1}{\epsilon} - c_3 \frac{1}{l} \right) \sim \mathcal{C} V_1 \left(\frac{1}{\epsilon} - c_3 \frac{1}{l} \right), \quad (14)$$

where $c_3 = 2\pi \left(\frac{\Gamma(\frac{3}{4})}{\Gamma(\frac{1}{4})} \right)^2$ is a constant as in AdS , stemming the finite cutoff-independent part of the integral. Note that here we have used the relation $\tau_{UV} = i\epsilon$ for the ultraviolet cutoff in

⁴Strictly speaking, this may be too restrictive. We have required $x(\tau)$ for all τ be real-valued: this means that each point on the surface directly maps to a corresponding real-valued spatial location within the strip in the dual CFT_3 . One might instead think that one need only require the boundary value $x(0)$ be real, which would not restrict the τ -path. This would suggest more general complex extremal surfaces defined over complex τ -space, with the width Δx required to be real-valued. See *e.g.* [23] for some discussions along these lines: I thank S. Fischetti for a discussion on this point.

the dual Euclidean field theory, suggested by previous investigations⁵ in dS/CFT . Also we have rewritten the last expression in (14) in terms of the dS_4/CFT_3 central charge $\mathcal{C}_3 \sim -\frac{R_{dS}^2}{G_4}$ appearing in the $\langle TT \rangle$ correlators in [3], reviewed above. S_{dS} in (14) is real-valued and bears structural resemblance to entanglement entropy in a dual CFT_3 with central charge $\mathcal{C}_3 \sim -\frac{R_{dS}^2}{G_4} < 0$. The first term resembles an area law divergence [32, 33], proportional to the area of the interface between the subregion and the environment, in units of the ultraviolet cutoff. It is also proportional to the central charge which represents the number of degrees of freedom in the dual CFT: in this case, $\mathcal{C} < 0$ reflecting the fact that the CFT is non-unitary. The second term is a finite cutoff independent piece. Whether the expression (14) physically is holographic entanglement entropy in dS_4/CFT_3 is less clear from this bulk extremal surface analysis.

In some sense, $-S_{dS}$ appears to resemble entanglement entropy in AdS/CFT , sharing various features including subadditivity. For instance, the quantity $I_{dS}[A, B] = S_{dS}[A] + S_{dS}[B] - S_{dS}[A \cup B]$ for two disjoint subsystems A, B , exhibits various properties of holographic mutual information in AdS including an analog of the disentangling transition in the classical gravity approximation [34], but with some crucial differences. For strip subregions that are sufficiently nearby but disjoint, $I_{dS}[A, B]$ is nonzero: *e.g.* using (14) for a single strip, we obtain for two parallel strips of equal width l and separation x ,

$$I_{dS}[A, B] = S_{dS}[A] + S_{dS}[B] - S_{dS}[A \cup B] \sim -\frac{R_{dS}^2}{G_4} c_3 V_1 \left(-\frac{2}{l} + \frac{1}{x} + \frac{1}{2l+x} \right). \quad (15)$$

$S_{dS}[A \cup B]$ arises from the area of the connected surface between A, B as $S(2l+x) + S(x)$. This is similar to the structure of holographic mutual information for strips in AdS_4 , *e.g.* the UV divergent pieces cancel, with a cutoff-independent divergence $\mathcal{C} \frac{V_1}{x}$ as the subregions collide. The striking difference is that $I_{dS}[A, B] \leq 0$, rather than positive definite, following from the fact that $\mathcal{C} = -\frac{R_{dS}^2}{G_4} < 0$. Thus $I_{dS}[A, B]$ is large and negative when the subregions are nearby, then increases as the separation $\frac{x}{l}$ increases, and eventually approaches zero as $\frac{x}{l} \rightarrow \frac{\sqrt{5}-1}{2} \sim 0.62$. Beyond this critical value, $I_{dS}[A, B]$ vanishes identically and the two subregions are disconnected. This disentangling transition in the classical gravity approximation arises from the transition between the connected and disconnected surface for $A \cup B$. What we are seeing is that $S_{dS}[A] + S_{dS}[B] \leq S_{dS}[A \cup B]$, *i.e.* $-S_{dS}$ satisfies strong subadditivity for disjoint parallel strips A, B . By comparison, using the real lightcone wedge surfaces in the previous

⁵See *e.g.* [3, 5, 4, 11], which discuss this (in some cases implicitly). Heuristically, we expect that evolution in the bulk direction is encoded by renormalization group flow in the dual field theory: see *e.g.* [24, 25, 26, 27, 28, 29] and more recently *e.g.* [30, 31] for discussions on this in the AdS context. In the present dS case, the bulk description is time evolution $i\frac{\delta\Psi}{\delta\tau} = \mathcal{H}\Psi$, with \mathcal{H} being an evolution operator. Through dS/CFT , this becomes $i\frac{\delta Z_{CFT}}{\delta\tau} = \mathcal{H}Z_{CFT}$. Heuristically this maps to a renormalization group equation schematically of the form $\frac{\delta Z_{CFT}}{\delta\epsilon} = \mathcal{O}Z_{CFT}$, if $\tau_{UV} = i\epsilon$, with \mathcal{O} an appropriate operator generating RG flow. If we view ϵ as a floating RG parameter, this again suggests the path $\tau = iT$ in complex τ -space for a dS/CFT interpretation.

subsection, we see that disjoint boundary subregions are always causally disconnected and thus uncorrelated for any nonzero separation. Correlation functions are nonzero: the disentangling transition above is in the classical gravity approximation, and we expect subleading terms in a large- N -like expansion of $I_{dS}[A, B]$ (see *e.g.* [35] in the AdS context).

We now discuss dS_{d+1} for even d (in particular dS_3, dS_5) where the nature of these extremal surfaces is different. We would like to retain the relation $\tau_{UV} = i\epsilon$ as following quite generally in dS/CFT from time evolution mapping to renormalization group flow. This suggests we parametrize the bulk time parameter τ along a complex path $\tau = iT$ as in dS_4 . However now with $A^2 > 0$ the surface (11) near $\tau \rightarrow 0$ gives $\dot{x} \sim \pm iA\tau^{d-1}$, *i.e.* $x(\tau) \sim \pm iA\tau^d$. Thus x cannot be made real-valued for any even d in this manner. A way out is to take the parameter $A^2 \rightarrow -A^2$: the surface equation now is the same as (5) but with the bulk time parametrized as $\tau = iT$. The expressions (10), (11) then give

$$\dot{x}^2 = \frac{A^2\tau^{2d-2}}{1 + A^2\tau^{2d-2}}, \quad S_{dS} = -i \frac{R_{dS}^{d-1}}{4G_{d+1}} V_{d-2} \int_{\tau_{UV}}^{\tau_*} \frac{d\tau}{\tau^{d-1}} \frac{2}{\sqrt{1 + A^2\tau^{2d-2}}} \\ \xrightarrow{\tau=iT} i^{1-d} \frac{R_{dS}^{d-1}}{2G_{d+1}} V_{d-2} \int_{\epsilon}^{T_*} \frac{dT}{T^{d-1}} \frac{1}{\sqrt{1 + (-1)^{d-1} A^2 T^{2d-2}}}. \quad (16)$$

For even d , the $(-1)^{d-1}$ gives rise to a ‘‘turning point’’ at $T_*^{2d-2} A^2 = 1$: the width now scales as $l \sim T_* \sim -iT_*$. The integral is as in AdS , giving

$$S_{dS} \sim i^{1-d} \frac{R_{dS}^{d-1}}{2G_{d+1}} V_{d-2} \left(\frac{1}{\epsilon^{d-2}} - c_d \frac{1}{l^{d-2}} \right). \quad (17)$$

The leading divergence $S_{dS}^{div} \sim i^{1-d} \frac{R_{dS}^{d-1}}{2G_{d+1}} \frac{V_{d-2}}{\epsilon^{d-2}}$ resembles an area law: the central charges $\mathcal{C}_d \sim i^{1-d} \frac{R_{dS}^{d-1}}{G_{d+1}}$ here resemble those in the $\langle TT \rangle$ correlators in [3] reviewed above. This leading behaviour appears independent of the shape of the subregion, expanding (10) and assuming that \dot{x} is small near the boundary τ_{UV} . Unlike dS_4 , note that S_{dS} in dS_{d+1} with even d is not real-valued, in particular for dS_3, dS_5 . For instance, in dS_3 , we obtain from (16)

$$\tau = iT, \quad x(\tau) \sim \pm \frac{1}{A} \sqrt{1 + A^2\tau^2}, \quad S_{dS} \sim -i \frac{R_{dS}}{G_3} \log \frac{\tau_*}{\tau_{UV}} = -i \frac{R_{dS}}{G_3} \log \frac{l}{\epsilon}. \quad (18)$$

Note that $x(\tau)$ appears real, although the parametrization is $\tau = iT$.

It is interesting to recall the Ryu-Takayanagi expression for entanglement entropy for an (infinitely long) strip-shaped subsystem with width along the x -direction, given as the area of the corresponding minimal surface in the bulk AdS_{d+1} geometry (with radius R),

$$S_{AdS}[R, x(r), r] = \frac{R^{d-1}}{4G_{d+1}} V_{d-2} \int \frac{dr}{r^{d-1}} \sqrt{1 + \left(\frac{dx}{dr} \right)^2}, \quad (x')^2 = \frac{A^2 r^{2d-2}}{1 - A^2 r^{2d-2}}, \quad (19)$$

where the conserved quantity A in the extremization is related to the turning point as $r_*^{d-1} = \frac{1}{A}$. Noting that dS_{d+1} in Poincare slicing (3) is just the analytic continuation of the corresponding $t = \text{constant}$ spatial slice in AdS_{d+1} , obtained by (2), *i.e.* $r \rightarrow -i\tau$, $t \rightarrow -iw$, $R \rightarrow -iR_{dS}$, let us carry out this analytic continuation on the Ryu-Takayanagi expression. Indeed we see that S_{dS} in (4) appears very much like the analytic continuation of $S_{AdS}[x(r), r]$, with the various factors of i conspiring to leave a single i behind, *i.e.*

$$S_{AdS}[R, x(r), r] \rightarrow -i \frac{R_{dS}^{d-1}}{4G_{d+1}} V_{d-2} \int \frac{d\tau}{\tau^{d-1}} \sqrt{1 - \left(\frac{dx}{d\tau}\right)^2} = S_{dS}[R_{dS}, x(\tau), \tau]. \quad (20)$$

On the analytic continuation of the extremization itself, we obtain

$$\begin{aligned} -\dot{x}^2 &= \frac{(-i)^{2d-2} A^2 \tau^{2d-2}}{1 - (-i)^{2d-2} A^2 \tau^{2d-2}}, \quad \text{i.e.} \quad \dot{x}^2 = \frac{-(-1)^{d-1} A^2 \tau^{2d-2}}{1 - (-1)^{d-1} A^2 \tau^{2d-2}}, \\ S_{dS} &= -i \frac{R_{dS}^{d-1}}{4G_{d+1}} V_{d-2} \int \frac{d\tau}{\tau^{d-1}} \frac{1}{\sqrt{1 - (-1)^{d-1} A^2 \tau^{2d-2}}}. \end{aligned} \quad (21)$$

This expression corroborates the minus sign in (16) and (13), (14). The analytic continuation essentially recovers our earlier calculations in dS_4 and dS_{d+1} for even d . For instance, in dS_5 (*i.e.* $d = 4$), we obtain

$$\dot{x}^2 = \frac{A^2 \tau^6}{1 + A^2 \tau^6}, \quad S_{dS} = -i \frac{R_{dS}^3}{4G_5} V_2 \int \frac{d\tau}{\tau^3} \frac{1}{\sqrt{1 + A^2 \tau^6}}. \quad (22)$$

With real A , this is as such a real extremal surface as in the previous subsection: taking A large minimises the area and we obtain the null surfaces earlier with vanishing area representing the past lightcone wedge of the subregion. However parametrizing as $\tau = iT$, there is a turning point at $\tau_* = \frac{i}{A^{1/3}}$, and a corresponding complex surface and corresponding area given by (16). The area in (22) then becomes $S_{dS} \sim i \frac{R_{dS}^3}{4G_5} V_2 (\frac{1}{\epsilon^2} - c_4 \frac{1}{l^2})$. The extra i can be thought of as arising from the odd powers of R_{dS} under the analytic continuation from AdS_5 . Thus interestingly for even d (in particular, dS_3 and dS_5), the expression S_{dS} obtained by analytic continuation of the Ryu-Takayanagi entanglement prescription leads to complex surfaces with corresponding area S_{dS} pure imaginary.

To summarize, we have studied bulk de Sitter codim-2 extremal surfaces. Real extremal surfaces are the boundaries of the past lightcone wedges of the boundary subregions, with vanishing area. Codim-2 complex extremal surfaces have area exhibiting structural resemblance with entanglement entropy in a dual CFT_d with $\mathcal{C}_d \sim i^{1-d} \frac{R_{dS}^{d-1}}{G_{d+1}}$ central charge⁶ matching those appearing in the $\langle TT \rangle$ correlators obtained from the wavefunction of the universe [3].

⁶Note that codim-1 surfaces with area functional $S \sim \frac{R_{dS}^d V_{d-1}}{l^d} \int \frac{d\tau}{\tau^d} \sqrt{\dot{x}^2 - 1}$ upon extremization exhibit area whose leading divergence does not reflect the CFT central charge.

In dS_4/CFT_3 , the area is real-valued and negative: in this sense, these complex surfaces have lower area, suggesting that they are the preferred minimal surfaces. Our calculations here have been done for a strip subregion but it would appear that generalizations to other subregion shapes will exhibit similar features. For instance, the spherical subregion extremal surface presumably exhibits a logarithmic term with interesting coefficient (this universal coefficient in the logarithmic term has been studied recently in [36], exhibiting agreement with the corresponding coefficient in the logarithmically divergent term in the wavefunction of the universe in the classical approximation).

It is worth noting that this analysis of bulk extremal surfaces is different from studies of entanglement entropy of bulk fields in de Sitter space *e.g.* [37, 38, 39, 40].

3 Extremal surfaces in the dS black brane

We now study extremal surfaces in the asymptotically dS spacetime studied in [13], *i.e.*

$$ds^2 = \frac{R_{dS}^2}{\tau^2} \left(-\frac{d\tau^2}{1 + \alpha\tau_0^d\tau^d} + (1 + \alpha\tau_0^d\tau^d)dw^2 + \sum_{i=1}^{d-1} dx_i^2 \right), \quad (23)$$

with α a complex phase and τ_0 is some real parameter of dimension length inverse. An analog of regularity in the interior for an asymptotically AdS solution is obtained here by a Wick rotation $\tau = il$ and demanding that the resulting spacetime (thought of as a saddle point in a path integral) in the interior approaches flat Euclidean space in the (l, w) -plane with no conical singularity. This makes the w -coordinate angular with fixed periodicity (and l is a radial coordinate), giving $\alpha = -(-i)^d$, $l \geq \tau_0$, $w \simeq w + \frac{4\pi}{(d-1)\tau_0}$. Thus the spacetime (23) is a complex metric which satisfies Einstein's equation with a positive cosmological constant $R_{MN} = \frac{d}{R_{dS}^2}g_{MN}$, $\Lambda = \frac{d(d-1)}{2R_{dS}^2}$. This resulting metric satisfying regularity is equivalent to one obtained by analytically continuing the Euclidean AdS black brane

$$ds^2 = \frac{R_{AdS}^2}{r^2} \left(\frac{dr^2}{1 - r_0^d r^d} + (1 - r_0^d r^d)d\theta^2 + \sum_{i=1}^{d-1} dx_i^2 \right), \quad (24)$$

where $\theta \sim \theta + \frac{4\pi}{(d-1)r_0}$, to the asymptotically de Sitter spacetime (23) using (2) and we identify $r_0 \equiv \tau_0$, giving the phase $\frac{-1}{(-i)^d}$. The regularity criterion is simply the analog of regularity of the $EAdS$ black brane. The condition $l \geq \tau_0$ is equivalent to the radial coordinate having the range $r \geq r_0$. We see that “normalizable” metric pieces are turned on in (23). We then expect a nonzero expectation value for the energy-momentum tensor here, as in the AdS context [41, 42, 28, 29]. In the present case [13], we have $T_{ij} = \frac{2}{\sqrt{h}} \frac{\delta Z_{CFT}}{\delta h^{ij}} = \frac{2}{\sqrt{h}} \frac{\delta \Psi}{\delta h^{ij}} \propto i \frac{R_{dS}^{d-1}}{G_{d+1}} g_{ij}^{(d)}$, where $g_{ij}^{(d)}$ is the coefficient of the normalizable τ^{d-2} term in the Fefferman-Graham expansion of the

metric (23). This definition of T_{ij} is natural for a CFT with partition function Z_{CFT} , equated with Ψ : thus, most notably, the i arising from Ψ , the wavefunction of the universe, implies that the energy-momentum tensor is real only if $g_{ij}^{(d)}$ is pure imaginary. In effect, this dS/CFT energy-momentum tensor can be thought of as the analytic continuation of the $EAdS$ one. The spacetime (23) for dS_4/CFT_3 gives real T_{ij} , with $T_{ww} = -\frac{R_{dS}^2}{G_4}\tau_0^3$ with $T_{ww} + (d-1)T_{ii} = 0$.

The w -coordinate is naturally interpreted as Euclidean time from the structure of the energy-momentum tensor: so let us now consider a strip subregion on a $w = \text{const}$ surface in (23). The area functional (in Planck units) of a bulk surface bounding this strip and dipping inwards is

$$S_{dS} = -i\frac{R_{dS}^{d-1}}{G_{d+1}}V_{d-2} \int \frac{d\tau}{\tau^{d-1}} \sqrt{\frac{1}{1 + \alpha\tau_0^d\tau^d} - \left(\frac{dx}{d\tau}\right)^2}, \quad (25)$$

defined so that for $\tau_0 = 0$, this reduces to our de Sitter discussion in sec. 2.2. For the dS_4 brane (*i.e.* $d = 3$), we obtain for the extremization,

$$\frac{\Delta x}{2} = \int_0^{\tau_*} \frac{iA\tau^2 d\tau}{\sqrt{(1 - i\tau_0^3\tau^3)(1 - A^2\tau^4)}}, \quad S = -i\frac{V_1 R_{dS}^2}{4G_4} \int_{\tau_{UV}}^{\tau_*} \frac{d\tau}{\tau^2} \frac{2}{\sqrt{(1 - i\tau_0^3\tau^3)(1 - A^2\tau^4)}}. \quad (26)$$

Now for small width l , this is essentially similar to the previous discussion on pure dS_4 and we have $\frac{i\Delta x}{2} \equiv \frac{il}{2} \sim \tau_* = \frac{i}{\sqrt{A}}$, where A is real. In particular, the width Δx being real-valued suggests that τ parametrizes a complex path $\tau = iT$ with T real. As l increases however, the other denominator approaches a zero also, with $\tau \rightarrow \frac{i}{\tau_0}$. In this limit, we thus have $\tau_* \rightarrow \frac{i}{\sqrt{A}} \sim \frac{i}{\tau_0}$ and large $l \sim -i\tau_*$, obtained from the double zero as

$$\frac{\Delta x}{2} = \frac{l}{2} \sim \int_0^{\tau_*} \frac{iA\tau^2 d\tau}{\sqrt{(1 - i\tau_0^3\tau^3)(1 - A^2\tau^4)}} \xrightarrow{\tau=iT} \int_0^{T_*} \frac{i\cdot i^3 AT_*^2 dT}{\sqrt{(1 - \tau_0^3 T^3)(1 - A^2 T^4)}}. \quad (27)$$

Note that reality of the width Δx implies now that the range of T is restricted as $T \leq \frac{1}{\tau_0}$ *i.e.* asymptotically $\tau \rightarrow \frac{i}{\tau_0}$. This is similar to the fact that in the AdS black brane, static minimal surfaces in the IR limit (large subsystem width) wrap the horizon but do not penetrate beyond.

Now the area integral exhibits a cutoff-independent piece which can be estimated from the contribution in the deep interior where $\tau \rightarrow \tau_*$: the contribution to the integral near the double zero thus scales as $i\Delta x$ giving

$$S^{fin} \sim -i\frac{V_1 R_{dS}^2}{G_4} \frac{1}{\tau_*^2}(il) = -\frac{R_{dS}^2}{G_4} \tau_0^2 V_1 l \equiv CT_0^2 V_1 l, \quad (28)$$

which resembles an extensive thermal entropy in a 3-dim CFT with central charge $\mathcal{C} \sim -\frac{R_{dS}^2}{G_4}$ at temperature $T_0 \equiv \tau_0$. Note that $S^{fin} < 0$. In fact S^{fin} is the analytic continuation (2) of the horizon entropy $\frac{R_{AdS}^2}{G_4} \tau_0^2 V_1 l$ of the $EAdS_4$ black brane (24), which can be obtained as the horizon contribution from the partition function in the classical approximation.

We recall that the entanglement entropy area functional for the AdS_{d+1} black brane from the Ryu-Takayanagi prescription is $S = \frac{V_{d-2}R^{d-1}}{4G_{d+1}} \int \frac{dr}{r^{d-1}} \sqrt{(\partial_r x)^2 + \frac{1}{1-r_0^d r^d}}$, giving

$$(x')^2 = \frac{A^2 r^{2d-2}}{(1-r_0^d r^d)(1-A^2 r^{2d-2})}, \quad S = \frac{V_{d-2}R^{d-1}}{4G_{d+1}} \int_\epsilon^{r^*} \frac{dr}{r^{d-1}} \frac{2}{\sqrt{(1-r_0^d r^d)(1-A^2 r^{2d-2})}}. \quad (29)$$

Under the analytic continuation, we obtain

$$\begin{aligned} \dot{x}^2 &= \frac{-(-1)^{d-1} A^2 \tau^{2d-2}}{(1-(-i)^d \tau_0^d \tau^d)(1-(-1)^{d-1} A^2 \tau^{2d-2})}, \\ S &= \frac{V_{d-2}R_{dS}^{d-1}}{4G_{d+1}} \int_{\tau_{UV}}^{\tau^*} \frac{-id\tau}{\tau^{d-1}} \frac{2}{\sqrt{(1-(-i)^d \tau_0^d \tau^d)(1-(-1)^{d-1} A^2 \tau^{2d-2})}}. \end{aligned} \quad (30)$$

For generic dimension d , we see that S is not real, as in the earlier discussion with $\tau_0 = 0$.

3.1 The de Sitter bluewall

We now explore metrics of the form (23), but with the parameter $\alpha = -1$ here⁷, *i.e.*

$$ds^2 = \frac{R_{dS}^2}{\tau^2} \left(-\frac{d\tau^2}{1-\tau_0^d \tau^d} + (1-\tau_0^d \tau^d) dw^2 + dx_i^2 \right) \equiv \frac{R_{dS}^2}{\tau^2} \left(-\frac{d\tau^2}{f(\tau)} + f(\tau) dw^2 + dx_i^2 \right). \quad (31)$$

The w -coordinate here has the range $-\infty \leq w \leq \infty$. This spacetime [13] has a Penrose diagram shown in Figure 2 which resembles that of the AdS black brane rotated by $\frac{\pi}{2}$: there are two asymptotically dS universes (for $\tau \lesssim \frac{1}{\tau_0}$), and timelike singularities cloaked by Cauchy horizons at $\tau = \frac{1}{\tau_0}$, which “cross” at a bifurcation region. The Penrose diagram has many similarities with the interior of the Reissner-Nordstrom black hole (or wormhole). Late time infalling observers near the Cauchy horizon see incoming lighttrays from early times as highly blueshifted, essentially stemming from lighttrays “crowding” near the Cauchy horizon, suggesting an instability. It is unclear if this spacetime has any interpretation in dS/CFT : nevertheless, formally, one finds the energy-momentum T_{ij} to be imaginary in dS_4/CFT_3 , perhaps reflecting the blueshift instability here. Here we will simply look for bulk codim-2 extremal surfaces, lying either on a $w = const$ slice or an $x = const$ slice (from a bulk point of view alone, either could be taken as Euclidean time slices), restricting to real surfaces which may also be timelike.

The area functional for a surface in (31) bounding a subregion on a $x = const$ slice of \mathcal{I}^+ , and wrapping the other $x_i \neq x$, is

$$S = \frac{R_{dS}^{d-1}}{4G_{d+1}} V_{d-2} \int \frac{d\tau}{\tau^{d-1}} \sqrt{\frac{1}{f(\tau)} - f(\tau) \left(\frac{dw}{d\tau} \right)^2}, \quad f(\tau) = 1 - \tau_0^d \tau^d. \quad (32)$$

⁷The metric (23) with $\alpha = +(-i)^d$ is similar to the dS black brane, except with T_{ij} of the opposite sign, while $\alpha = +1$ gives a real spacetime with a spacelike singularity at $\tau \rightarrow \infty$.

This does not correspond to any analytic continuation from the Ryu-Takayanagi formula for the AdS_4 black brane, so we analyse this directly focussing on the dS_4 bluewall. Along our earlier discussions in sec. 2, we find real extremal surfaces corresponding to

$$\dot{w}^2 = \frac{1}{(1 - \tau_0^3 \tau^3)^2} \frac{B^2 \tau^4}{1 - \tau_0^3 \tau^3 + B^2 \tau^4}, \quad S = \frac{V_1 R_{dS}^2}{4G_4} \int \frac{d\tau}{\tau^{d-1}} \frac{1}{\sqrt{1 - \tau_0^3 \tau^3 + B^2 \tau^4}}, \quad (33)$$

where the constant B arises from a conserved quantity in the extremization. The first equation describing the surface can be rewritten as

$$d\tau_* \equiv \frac{d\tau}{1 - \tau_0^3 \tau^3}, \quad \left(\frac{dw}{d\tau_*}\right)^2 \equiv (w'_*)^2 = \frac{B^2 \tau^4}{1 - \tau_0^3 \tau^3 + B^2 \tau^4}, \quad (34)$$

where we are using τ_* here for the ‘‘tortoise’’ coordinate in this bluewall geometry [13], analogous to the Schwarzschild tortoise coordinate r_* . Parametrized thus, we see as in the dS_4 case that increasing B decreases the area, as long as we restrict the surface to lie within the future asymptotic universe I , *i.e.* $f(\tau) > 0$. As $B^2 \rightarrow \infty$, these extremal surfaces become null with $(w'_*)^2 = 1$, corresponding to the past lightcone wedges of the boundary subregion, and have vanishing area. Thus extremal surfaces for a given subregion at \mathcal{I}^+ can be constructed as in dS_4 (Figure 1) by joining two half-extremal surfaces: this is the blue wedge in region I in Figure 2 (the half-surface when not cut off continues as a null surface through the Cauchy horizon into region III , represented by the dotted extension of the blue line). As the subregion grows in size, this blue wedge approaches and eventually wraps the future Cauchy horizons.

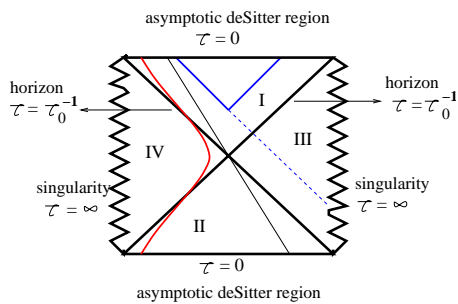


Figure 2: de Sitter ‘‘bluewall’’ Penrose diagram and some extremal surfaces with at least one end anchored at \mathcal{I}^+ . The blue wedge is null, while the red timelike surface goes from \mathcal{I}^+ to \mathcal{I}^- .

One might imagine that there are timelike surfaces which are not restricted to just region I but instead start on \mathcal{I}^+ in I and cross over to II ending on the past boundary \mathcal{I}^- . These can be found with the parameter $B^2 > 0$ being finite. In this case, we see that $(w'_*)^2 \rightarrow 0$ as $\tau \rightarrow 0$ and $(w'_*)^2 \rightarrow 1$ as $\tau \rightarrow \frac{1}{\tau_0}$ near the horizon in I . Now after the surface crosses the future Cauchy horizon, we have $f(\tau) < 0$ in IV . Requiring that $(w'_*)^2$ in (34) satisfies $(w'_*)^2 \geq 0$ corresponding to real surfaces, it is possible to see (*e.g.* by plotting as a function of $\tau_0 \tau$) that the parameter B^2 is bounded below by a critical value. There is a family of such surfaces: we will isolate one ‘‘critical’’ surface for a particular value of B , in what follows. Drawing analogies with the study

of the phase transition found in [43] (although the physical context there is different), we note that $(w'_*)^2 \rightarrow \infty$ when the denominator in (34) approaches a double zero (with $y \equiv \tau_0\tau$), *i.e.*

$$1 - y_c^3 + \frac{B^2}{\tau_0^4} y_c^4 = 0, \quad -3y_c^2 + 4\frac{B^2}{\tau_0^4} y_c^3 = 0 \quad \Rightarrow \quad \frac{B^2}{\tau_0^4} = \frac{3}{4.4^{1/3}}, \quad y_c = 4^{1/3}. \quad (35)$$

This corresponds to $\tau_c = \frac{4^{1/3}}{\tau_0} \sim \frac{1.6}{\tau_0}$ which is just a little inside the Cauchy horizon in region *IV*. Note that $(w'_*)^2|_{\tau_c} \rightarrow \infty$ here means this curve is normal to the $w = \text{const}$ line here (these are straight spacelike lines passing through the bifurcation point and hitting the singularity in *IV*), or equivalently tangent to the $\tau = \text{const}$ curve at τ_c in *IV*. The corresponding surface from $\tau = 0$ to $\tau = \tau_c$ can be drawn as a curve in the (τ, w) -plane: it can be joined smoothly at τ_c with a corresponding curve from \mathcal{I}^- , resulting approximately in the red curve in Figure 2. This surface crosses the upper and lower Cauchy horizons at $\tau = \frac{1}{\tau_0}, w = +\infty$ and $\tau = \frac{1}{\tau_0}, w = -\infty$. The area of this surface has a leading divergence $S \sim \frac{R_{dS}^2}{G_4} \frac{V_1}{\tau_{UV}}$. Near the double zero, Δw acquires a large contribution and we can estimate $S \sim \frac{R_{dS}^2}{G_4} V_1 \Delta w$. This surface is vaguely reminiscent of the extremal surface in [44] which goes from one timelike boundary to the other: since the dS bluewall metric itself is related to the AdS-Schwarzschild black brane by flipping minus signs, it is perhaps not surprising that there exists a similar surface here (but timelike), albeit with no obvious corresponding interpretation. In light of ER=EPR [45], it is amusing to speculate that the subregion here corresponds to copies on both \mathcal{I}^\pm possibly “entangled”, in some sense, thinking of the bluewall geometry as a “timelike wormhole” with the bifurcation region being the Einstein Rosen bridge. Note however that strictly speaking, all timelike geodesics go from \mathcal{I}^- to \mathcal{I}^+ (unlike a shortcut in spacetime) either through the bifurcation region or through the Cauchy horizons, subject to the blueshift instability [13].

With a $w = \text{const}$ slice, real extremal surfaces likewise have

$$\dot{x}^2 = \frac{B^2\tau^4}{(1 - \tau_0^3\tau^3)(1 + B^2\tau^4)}, \quad S = \frac{V_1 R_{dS}^2}{4G_4} \int_{\tau_{UV}}^{\tau_0} \frac{d\tau}{\tau^2} \frac{2}{\sqrt{(1 - \tau_0^3\tau^3)(1 + B^2\tau^4)}}. \quad (36)$$

For $B^2 \rightarrow \infty$, these are again null extremal surfaces $\dot{x}^2 = \frac{1}{1 - \tau_0^3\tau^3}$ with vanishing area. These surfaces all lie on a $w = \text{const}$ slice (thin black straight line from \mathcal{I}^+ to \mathcal{I}^- in Figure 2).

4 Discussion

We have considered extremal surfaces in bulk de Sitter space (in the Poincare slicing) on constant boundary Euclidean time slices bounding subregions at future timelike infinity, motivated by the Ryu-Takayanagi prescription for entanglement entropy in *AdS/CFT*. Stemming from certain crucial sign differences, we have seen real extremal surfaces which are essentially the

restrictions of the boundaries of the past lightcone wedges of the subregion: these are null surfaces with vanishing area. We have also seen complex extremal surfaces which do not always have real-valued area: this has parallels with analytically continuing from the Ryu-Takayanagi formula in AdS . In dS_4 , the area is real-valued and negative. The area has structural resemblance with entanglement entropy in a dual CFT_d , with the leading divergence of the form $\mathcal{C}_d \frac{V_{d-2}}{\epsilon^{d-2}}$: the central charges $\mathcal{C}_d \sim i^{1-d} \frac{R_{dS}^{d-1}}{G_{d+1}}$ here resemble those in the CFT energy-momentum tensor $\langle TT \rangle$ correlators in [3] obtained in dS/CFT using $Z_{CFT} = \Psi$ and a semiclassical approximation $\Psi \sim e^{iS_{cl}}$ for the wavefunction of the universe. Alternatively, the strip entanglement entropy of a nonunitary CFT with these central charges would be of this form (assuming it exists), which the area of these complex extremal surfaces reproduces. This appears distinct from bulk entanglement entropy in de Sitter space (from a bulk density matrix via the wavefunction Ψ). We have also studied extremal surfaces in the dS black brane (where there is a finite cutoff-independent extensive piece), and the related dS bluewall spacetime. It is worth mentioning that there may exist other extrema of the area functional: for instance, we have required that $x(\tau)$ parametrizing the strip width be real-valued, which suggests the path $\tau = iT$ in complex τ -space. This appears consistent with possible dS/CFT interpretations and also corroborates with our discussion of the dS black brane. However this may be restrictive and more general complex extremal surfaces may be relevant in complex τ -space (see *e.g.* [23]). It may be interesting to understand if the analysis of [18] can be applied in this case to obtain insights into extremal surfaces.

While this analysis of bulk extremal surfaces could be regarded as simply a study of certain kinds of probes of asymptotically de Sitter spaces, it cannot pinpoint whether the corresponding area is expected to have a physical interpretation as entanglement entropy in the dual CFT, although the results do appear so, keeping in mind the central charges of the non-unitary CFTs in question. It is tempting to study this in light of the higher spin dS_4/CFT_3 duality of [4]. However the presence of massless higher spin fields might suggest that extremal surfaces which are geometric gravitational objects are not accurate (see *e.g.* [46, 47] which study entanglement entropy from Wilson lines in higher spin AdS holography). Nevertheless it is interesting to ask if these extremal surfaces have significance in some approximation where the higher spin symmetry is not exact. In this case, it would be interesting to explore the physical interpretation here more directly from a Euclidean CFT_3 point of view. One way to think about entanglement entropy in field theory (lattice models) is in terms of the eigenvalues of a correlation matrix and a corresponding von Neumann entropy (see *e.g.* [48] and more recently [49]). In that context, a simple model of a massless scalar field with wrong sign kinetic terms might suggest that the correlation matrix squared C^2 is related to that for an ordinary massless scalar field by a minus sign, so that C -eigenvalues λ_k become $i\lambda_k$. Then the associated von Neumann entropy is in general not real-valued: it would be interesting to understand this better.

Acknowledgements: It is a pleasure to thank the participants of the “Entanglement from Gravity” Discussion meeting, ICTS, Bangalore, in particular S. Banerjee, G. Mandal and R. Myers for helpful comments. I also thank the organizers of this workshop and the Indian Strings Meeting 2014, Puri, for hospitality as this was being completed. This work is partially supported by a grant to CMI from Infosys Foundation.

References

- [1] A. Strominger, “The dS / CFT correspondence,” JHEP **0110**, 034 (2001) [hep-th/0106113].
- [2] E. Witten, “Quantum gravity in de Sitter space,” [hep-th/0106109].
- [3] J. M. Maldacena, “Non-Gaussian features of primordial fluctuations in single field inflationary models,” JHEP **0305**, 013 (2003), [astro-ph/0210603].
- [4] D. Anninos, T. Hartman and A. Strominger, “Higher Spin Realization of the dS/CFT Correspondence,” arXiv:1108.5735 [hep-th].
- [5] D. Harlow and D. Stanford, “Operator Dictionaries and Wave Functions in AdS/CFT and dS/CFT,” arXiv:1104.2621 [hep-th].
- [6] G. S. Ng and A. Strominger, “State/Operator Correspondence in Higher-Spin dS/CFT,” Class. Quant. Grav. **30**, 104002 (2013) [arXiv:1204.1057 [hep-th]].
- [7] D. Anninos, “De Sitter Musings,” Int. J. Mod. Phys. A **27**, 1230013 (2012) [arXiv:1205.3855 [hep-th]].
- [8] D. Das, S. R. Das, A. Jevicki and Q. Ye, “Bi-local Construction of Sp(2N)/dS Higher Spin Correspondence,” JHEP **1301**, 107 (2013) [arXiv:1205.5776 [hep-th]].
- [9] D. Anninos, F. Denef and D. Harlow, “The Wave Function of Vasiliev’s Universe - A Few Slices Thereof,” Phys. Rev. D **88**, 084049 (2013) [arXiv:1207.5517 [hep-th]].
- [10] D. Anninos, F. Denef, G. Konstantinidis and E. Shaghoulian, “Higher Spin de Sitter Holography from Functional Determinants,” arXiv:1305.6321 [hep-th].
- [11] D. Das, S. R. Das and G. Mandal, “Double Trace Flows and Holographic RG in dS/CFT correspondence,” arXiv:1306.0336 [hep-th].
- [12] S. Banerjee, A. Belin, S. Hellerman, A. Lepage-Jutier, A. Maloney, j. j. Radievi and S. Shenker, “Topology of Future Infinity in dS/CFT,” JHEP **1311**, 026 (2013) [arXiv:1306.6629 [hep-th]].
- [13] D. Das, S. R. Das and K. Narayan, “dS/CFT at uniform energy density and a de Sitter ’bluewall’,” JHEP **1404**, 116 (2014) [arXiv:1312.1625 [hep-th]].
- [14] S. Ryu and T. Takayanagi, “Holographic derivation of entanglement entropy from AdS/CFT,” Phys. Rev. Lett. **96**, 181602 (2006) [hep-th/0603001].
- [15] S. Ryu and T. Takayanagi, “Aspects of Holographic Entanglement Entropy,” JHEP **0608**, 045 (2006) [hep-th/0605073].

- [16] T. Nishioka, S. Ryu and T. Takayanagi, “Holographic Entanglement Entropy: An Overview,” *J. Phys. A* **42** (2009) 504008;
- [17] T. Takayanagi, “Entanglement Entropy from a Holographic Viewpoint,” *Class. Quant. Grav.* **29** (2012) 153001 [arXiv:1204.2450 [gr-qc]].
- [18] A. Lewkowycz and J. Maldacena, “Generalized gravitational entropy,” *JHEP* **1308**, 090 (2013) [arXiv:1304.4926 [hep-th]].
- [19] V. E. Hubeny, M. Rangamani and T. Takayanagi, “A Covariant holographic entanglement entropy proposal,” *JHEP* **0707** (2007) 062 [arXiv:0705.0016 [hep-th]].
- [20] V. E. Hubeny and M. Rangamani, “Causal Holographic Information,” *JHEP* **1206**, 114 (2012) [arXiv:1204.1698 [hep-th]].
- [21] L. Fidkowski, V. Hubeny, M. Kleban and S. Shenker, “The Black hole singularity in AdS / CFT,” *JHEP* **0402**, 014 (2004) [hep-th/0306170].
- [22] S. Fischetti and D. Marolf, “Complex Entangling Surfaces for AdS and Lifshitz Black Holes?,” *Class. Quant. Grav.* **31**, no. 21, 214005 (2014) [arXiv:1407.2900 [hep-th]].
- [23] S. Fischetti, D. Marolf and A. Wall, “A paucity of bulk entangling surfaces: AdS wormholes with de Sitter interiors,” arXiv:1409.6754 [hep-th].
- [24] E. T. Akhmedov, “A Remark on the AdS / CFT correspondence and the renormalization group flow,” *Phys. Lett. B* **442**, 152 (1998) [hep-th/9806217].
- [25] E. Alvarez and C. Gomez, “Geometric holography, the renormalization group and the c theorem,” *Nucl. Phys. B* **541**, 441 (1999) [hep-th/9807226].
- [26] D. Z. Freedman, S. S. Gubser, K. Pilch and N. P. Warner, “Renormalization group flows from holography supersymmetry and a c theorem,” *Adv. Theor. Math. Phys.* **3**, 363 (1999) [hep-th/9904017].
- [27] J. de Boer, E. P. Verlinde and H. L. Verlinde, “On the holographic renormalization group,” *JHEP* **0008**, 003 (2000) [hep-th/9912012].
- [28] S. de Haro, S. N. Solodukhin and K. Skenderis, “Holographic reconstruction of spacetime and renormalization in the AdS/CFT correspondence,” *Commun. Math. Phys.* **217**, 595 (2001) [arXiv:hep-th/0002230].
- [29] K. Skenderis, “Lecture notes on holographic renormalization,” *Class. Quant. Grav.* **19**, 5849 (2002) [arXiv:hep-th/0209067].
- [30] I. Heemskerk and J. Polchinski, “Holographic and Wilsonian Renormalization Groups,” *JHEP* **1106**, 031 (2011) [arXiv:1010.1264 [hep-th]].
- [31] T. Faulkner, H. Liu and M. Rangamani, “Integrating out geometry: Holographic Wilsonian RG and the membrane paradigm,” *JHEP* **1108**, 051 (2011) [arXiv:1010.4036 [hep-th]].
- [32] L. Bombelli, R. K. Koul, J. Lee and R. D. Sorkin, “A Quantum Source of Entropy for Black Holes,” *Phys. Rev. D* **34** (1986) 373.

- [33] M. Srednicki, “Entropy and area,” *Phys. Rev. Lett.* **71** (1993) 666 [hep-th/9303048].
- [34] M. Headrick, “Entanglement Renyi entropies in holographic theories,” *Phys. Rev. D* **82**, 126010 (2010) [arXiv:1006.0047 [hep-th]].
- [35] T. Faulkner, A. Lewkowycz and J. Maldacena, “Quantum corrections to holographic entanglement entropy,” *JHEP* **1311**, 074 (2013) [arXiv:1307.2892].
- [36] K. Narayan, “de Sitter space and extremal surfaces for spheres,” arXiv:1504.07430 [hep-th].
- [37] J. Maldacena and G. L. Pimentel, “Entanglement entropy in de Sitter space,” *JHEP* **1302**, 038 (2013) [arXiv:1210.7244 [hep-th]].
- [38] S. Kanno, J. Murugan, J. P. Shock and J. Soda, “Entanglement entropy of α -vacua in de Sitter space,” *JHEP* **1407**, 072 (2014) [arXiv:1404.6815 [hep-th]].
- [39] N. Iizuka, T. Noumi, N. Ogawa, “Entanglement Entropy of deSitter Space α -Vacua,” arXiv:1404.7487[hep-th].
- [40] W. Fischler, S. Kundu and J. F. Pedraza, “Entanglement and out-of-equilibrium dynamics in holographic models of de Sitter QFTs,” *JHEP* **1407**, 021 (2014) [arXiv:1311.5519 [hep-th]].
- [41] V. Balasubramanian and P. Kraus, “A stress tensor for anti-de Sitter gravity,” *Commun. Math. Phys.* **208**, 413 (1999) [arXiv:hep-th/9902121].
- [42] R. C. Myers, “Stress tensors and Casimir energies in the AdS/CFT correspondence,” *Phys. Rev. D* **60**, 046002 (1999) [arXiv:hep-th/9903203].
- [43] K. Narayan, T. Takayanagi and S. P. Trivedi, “AdS plane waves and entanglement entropy,” *JHEP* **1304**, 051 (2013) [arXiv:1212.4328 [hep-th]].
- [44] T. Hartman and J. Maldacena, “Time Evolution of Entanglement Entropy from Black Hole Interiors,” *JHEP* **1305**, 014 (2013) [arXiv:1303.1080 [hep-th]].
- [45] J. Maldacena and L. Susskind, “Cool horizons for entangled black holes,” *Fortsch. Phys.* **61**, 781 (2013) [arXiv:1306.0533 [hep-th]].
- [46] J. de Boer and J. I. Jottar, “Entanglement Entropy and Higher Spin Holography in AdS₃,” *JHEP* **1404**, 089 (2014) [arXiv:1306.4347 [hep-th]].
- [47] M. Ammon, A. Castro and N. Iqbal, “Wilson Lines and Entanglement Entropy in Higher Spin Gravity,” *JHEP* **1310**, 110 (2013) [arXiv:1306.4338 [hep-th]].
- [48] I. Peschel and V. Eisler, “Reduced density matrices and entanglement entropy in free lattice models”, *J.Phys.,A*42,504003 (2009), [arXiv:0906.1663 [cond-mat]].
- [49] C. P. Herzog and M. Spillane, “Tracing Through Scalar Entanglement,” *Phys. Rev. D* **87**, 025012 (2013) [arXiv:1209.6368 [hep-th]].